







On the Possibility of GW190425 Being a Black Hole–Neutron Star Binary Merger

Koutarou Kyutoku^{1,2,3,4} , Sho Fujibayashi⁵, Kota Hayashi², Kyohei Kawaguchi⁶, Kenta Kiuchi^{2,5} , Masaru Shibata^{2,5} , and Masaomi Tanaka⁷ 

¹ Department of Physics, Kyoto University, Kyoto 606-8502, Japan

² Center for Gravitational Physics, Yukawa Institute for Theoretical Physics, Kyoto University, Kyoto 606-8502, Japan

³ Theory Center, Institute of Particles and Nuclear Studies, KEK, Tsukuba, Ibaraki 305-0801, Japan

⁴ Interdisciplinary Theoretical and Mathematical Sciences Program (iTHEMS), RIKEN, Wako, Saitama 351-0198, Japan

⁵ Max Planck Institute for Gravitational Physics (Albert Einstein Institute), Am Mühlenberg 1, Potsdam-Golm D-14476, Germany

⁶ Institute for Cosmic Ray Research, The University of Tokyo, 5-1-5 Kashiwanoha, Kashiwa, Chiba 277-8582, Japan

⁷ Astronomical Institute, Tohoku University, Aoba, Sendai 980-8578, Japan

Received 2020 January 16; revised 2020 January 21; accepted 2020 January 21; published 2020 February 6

Abstract

We argue that the kilonova/macronova associated with the gravitational-wave event GW190425 could have been bright enough to be detected if it was caused by the merger of a low-mass black hole (BH) and a neutron star (NS). Although tidal disruption occurs for such a low-mass BH is generally expected, the masses of the dynamical ejecta are limited to $\lesssim 10^{-3} M_{\odot}$, which is consistent with previous work in the literature. The remnant disk could be as massive as $0.05\text{--}0.1 M_{\odot}$, and the disk outflow of $\sim 0.01\text{--}0.03 M_{\odot}$ is likely to be driven by viscous or magnetohydrodynamic effects. The disk outflow may not be neutron-rich enough to synthesize an abundance of lanthanide elements, even in the absence of strong neutrino emitter, if the ejection is driven on the viscous timescale of $\gtrsim 0.3$ s. If this is the case, the opacity of the disk outflow is kept moderate, and a kilonova/macronova at the distance of GW190425 reaches a detectable brightness of 20–21 mag at 1 day after merger for most viewing angles. If some disk activity ejects the mass within ~ 0.1 s, instead, lanthanide-rich outflows would be launched and the detection of emission becomes challenging. Future possible detections of kilonovae/macronovae from GW190425-like systems will disfavor the prompt collapse of binary NSs and a non-disruptive low-mass BH–NS binary associated with a small NS radius, whose mass ejection is negligible. The host-galaxy distance will constrain the viewing angle and deliver further information about the mass ejection.

Unified Astronomy Thesaurus concepts: Neutron stars (1108); Black holes (162); Gravitational wave sources (677); Compact binary stars (283); Time domain astronomy (2109)

1. Introduction

Gravitational-wave observations continue to refine our understanding of compact objects. The first event and subsequent detections of binary black-hole (BH) mergers revealed the ubiquity of massive BHs (Abbott et al. 2019a), some of which may be spinning rapidly (Venumadhav et al. 2019). The first detection of a binary neutron-star (NS) merger, GW170817 (Abbott et al. 2017c), followed by extensive electromagnetic observations (Abbott et al. 2017b, 2017d; Arcavi et al. 2017; Coulter et al. 2017; Goldstein et al. 2017; Lipunov et al. 2017; Savchenko et al. 2017; Soares-Santos et al. 2017; Tanvir et al. 2017; Valenti et al. 2017) delivered a wealth of information about supranuclear-density matter (e.g., Abbott et al. 2018a; De et al. 2018; Narikawa et al. 2019), gamma-ray bursts (e.g., Abbott et al. 2017b; Goldstein et al. 2017; Mooley et al. 2018), *r*-process elements (e.g., Kasen et al. 2017; Tanaka et al. 2017), the theory of gravitation (e.g., Abbott et al. 2017b, 2019b), and cosmological expansion (e.g., Abbott et al. 2017a), while their masses and spins are consistent with the Galactic population (Farrow et al. 2019).

The recent report of gravitational waves from a NS binary system with $\sim 3.4 M_{\odot}$, GW190425 (formerly S190425z), may change our understanding of the mass spectrum of compact objects (Abbott et al. 2020). As the total mass of Galactic binary NSs has been limited to $2.5\text{--}2.9 M_{\odot}$ (Farrow et al. 2019), this event represents a population that has never been found in the Galaxy as noted in Abbott et al. (2020), if it is genuinely a binary NS merger. The possible mass asymmetry

could add further value to this event, because NSs as massive as $\gtrsim 1.9 M_{\odot}$ have been found only in NS–white-dwarf binaries (e.g., Cromartie et al. 2020). On another front, the violation of the low-spin prior, with which dimensionless spin parameter is limited to ≤ 0.05 (Abbott et al. 2020), is not an issue for a BH. Indeed, if the lighter component is a NS with a typical mass of $1.35 M_{\odot}$, the heavy one is consistent with $\gtrsim 2 M_{\odot}$ and is not safely concluded to be a NS. If this heavy component is a low-mass BH, it challenges existence of the mass gap between BHs and NSs (Kreidberg et al. 2012; Özel et al. 2012). Thus, the determination of the binary type is essential to obtain robust astrophysical knowledge.

It is generally difficult to differentiate low-mass⁸ BH–NS binaries from binary NSs. In fact, even GW170817 and associated electromagnetic counterparts have not been strictly confirmed to be a binary NS merger (Coughlin & Dietrich 2019; Foucart et al. 2019; Hinderer et al. 2019). The distinction of the binary type becomes more difficult in the absence of electromagnetic counterparts.

Unfortunately, no plausible electromagnetic counterpart was detected with GW190425. This is because of either intrinsically dim emission or insufficient coverage of the huge error region (see Table 2 of Hosseinzadeh et al. 2019 for the compilation of relevant follow-up observations). Despite the poor localization of GW190425, however, the Global Relay of Observatories Watching Transients Happen network observed impressive

⁸ In this Letter, “low mass” means $\gtrsim 1.9 M_{\odot}$, for which the distinction from the NS is not trivial.

thousands of square degrees, which amount to 46% and 21% of the 90% probability region derived by BAYESTER and LALInference, respectively (Coughlin et al. 2019). Intriguingly, it is claimed in Pozanenko et al. (2019) that GRB 190425 coincident with GW190425 had come from the northern hemisphere covered by Coughlin et al. (2019). It would be worthwhile to investigate whether such an optical survey has sufficient discriminative power for future reference (see also Andreoni et al. 2019 and Coughlin et al. 2020 for related work on GW190425 as a binary NS merger and other gravitational-wave candidates).

In this Letter, we discuss whether GW190425 could have been identified unambiguously as a BH–NS binary or binary NSs, if follow-up observations like Coughlin et al. (2019) would have targeted the right sky location. We base our arguments on a suite of latest numerical-relativity simulations (K. Hayashi et al., in preparation, Fujibayashi et al. 2020) for the mass ejection and radiation-transfer simulations for the kilonova/macronova (Kawaguchi et al. 2019). Note that none of the simulations are tuned to reproduce this specific event, GW190425.

2. Gravitational Waves

First, we recall that gravitational-wave observations with the current sensitivity of detectors are unlikely to differentiate BH–NS binaries from binary NSs, whereas it is possible and concrete in principle.

2.1. Inspiral Phase

It is broadly recognized that gravitational waves from the inspiral phase are not useful to distinguish low-mass BH–NS binaries from binary NSs with current detectors (e.g., Hannam et al. 2013). The primary reason is the $\sim 99.9\%$ correlation between the mass ratio and the spin parameter (Cutler & Flanagan 1994). A precise determination of these degenerated parameters and an associated classification of binary types will become possible only when gravitational-wave detectors improve their sensitivity or multiband gravitational-wave astronomy is realized (Sesana 2016).

Even if the degeneracy is solved, it is intrinsically difficult to determine whether an object with $\gtrsim 2 M_{\odot}$ is a BH or a NS from our limited knowledge about the NS maximum mass (Shibata et al. 2019). Although tidal deformability and the spin-induced quadrupole parameter of a NS are different from those of a BH, their extraction is challenging (Harry & Hinder 2018). This is particularly the case for a NS near the maximum mass, where these values approach the BH limit (Yagi & Yunes 2013).

2.2. Merger Phase

Another possible method of distinction is to observe gravitational waves from the merger phase in detail. If the source is a low-mass BH–NS binary, tidal disruption of the NS suddenly shuts off gravitational-wave emission without exciting quasi-normal modes (Shibata et al. 2009). If the source is massive binary NSs with a total mass of $\sim 3.4 M_{\odot}$, the plausible merger outcome is the prompt collapse (Hotokezaka et al. 2011), and the ringdown emission from the remnant BH should accompany it. Our simulations indicate that this is also true for a highly asymmetric binary for which the light component is tidally disrupted (Kiuchi et al. 2019). The difference in

waveforms is evident for the case when a massive NS is formed.

However, the merger phase can be detected only with high sensitivity at high frequency. This is because the characteristic frequency of both tidal disruption and quasi-normal modes are in the kilohertz range (e.g., Shibata et al. 2009). Thus, gravitational waves are not likely to enable us to differentiate a low-mass BH–NS binary and binary NSs until the third-generation detectors come online.

3. Electromagnetic Counterpart

Next, we discuss whether electromagnetic counterparts allow us to distinguish a low-mass BH–NS binary and binary NSs for a GW190425-like event. Specifically, we focus on the observation of the kilonova/macronova down to ~ 21 mag at 1–2 days after merger in the r - and g -bands typically achieved in Coughlin et al. (2019). They also put an upper limit of ~ 15 mag in the J -band, but this is not restrictive in realistic situations.

3.1. Mass Ejection

The properties of the kilonova/macronova are determined by the ejected material (Li & Paczyński 1998). Thus, we begin with investigating the mass ejection from GW190425-like systems based on our numerical-relativity simulations. The ejection channels are usually separated into (hydro)dynamical processes working during merger and disk activity in the post-merger phase, and accordingly we discuss these two separately below.

First of all, we recall that no mass ejection is expected from symmetric⁹ binary NSs as massive as $\sim 3.4 M_{\odot}$, because they are highly likely to collapse promptly into a BH without leaving baryonic material (Kiuchi et al. 2010; Hotokezaka et al. 2013). Accordingly, no kilonova/macronova is expected for this case, and neither is a gamma-ray burst. This means that any non-detection will be consistent with massive binary NSs as far as the (nearly) equal-mass system is allowed by gravitational-wave observations. If a massive NS is formed transiently thanks to a large maximum mass, the BH–disk formation and mass ejection could be similar to those for asymmetric binaries (Kiuchi et al. 2019).¹⁰ Hereafter in this section, we focus on clarifying the similarity and difference between a low-mass BH–NS binary and asymmetric binary NSs.

3.1.1. Merger Phase

Coincidentally, we have recently simulated mergers of non-spinning $2 M_{\odot}$ BH– $1.35 M_{\odot}$ NS binaries, which reasonably model possible sources of GW190425 (K. Hayashi et al., in preparation). Data analysis of GW190425 indicates that the spin parameter is small (Abbott et al. 2020), and the neglect of the spin is acceptable. We adopted three piecewise polytropes, HB, H, and 1.25 H (Lackey et al. 2012),¹¹ with which NS radii took 11.6 km, 12.3 km, and 13.0 km, respectively. This range spans middle to large radii inferred by GW170817 (Abbott et al. 2018a) and should be sufficient to cover non-trivial outcomes of BH–NS binary mergers.

⁹ In this Letter, “symmetric” means the mass ratio of 0.9–1, where the precise threshold is admittedly ambiguous.

¹⁰ This scenario strongly indicates that the merger remnant of GW170817 survived for long period of time.

¹¹ 1.25H is denoted by $p6.0F3.0$ in Lackey et al. (2012).

Actual simulations are performed with the SACRA-MPI code (Yamamoto et al. 2008; Kiuchi et al. 2017) with three different resolutions to check numerical convergence. Because these merger simulations aim at deriving the amounts of dynamical ejecta and formed accretion disks, neutrino transport or magnetic fields are not incorporated (see below for post-merger simulations).

The masses of the dynamical ejecta are found to be as small as $<10^{-4} M_{\odot}$, $<10^{-4} M_{\odot}$, and $4 \times 10^{-4} M_{\odot}$ for HB, H, and 1.25H, respectively, although the NSs are disrupted violently to leave moderately massive disks of $0.04 M_{\odot}$, $0.07 M_{\odot}$, and $0.1 M_{\odot}$. The smallness of the dynamical ejecta in low-mass BH–NS binaries is consistent with the tendency found in our previous study (see Figure 11 of Kyutoku et al. 2015 and also Foucart et al. 2019). Although we did not incorporate neutrino transport in these simulations, previous studies confirmed that the dynamical ejecta are extremely neutron-rich for BH–NS binaries (Roberts et al. 2017; Kyutoku et al. 2018).

We have also simulated $1.8 M_{\odot}$ – $1.2 M_{\odot}$ mergers of BH–NS binaries and binary NSs with the APR4 equation of state (Akmal et al. 1998), with which the radius of a $1.2 M_{\odot}$ NS is 11.0 km, for comparing outcomes (K. Hayashi et al., in preparation). We find that (i) the mass of the disk, 0.07 – $0.08 M_{\odot}$, depends only weakly on the binary type, and (ii) the mass of the dynamical ejecta is $9 \times 10^{-4} M_{\odot}$ for asymmetric binary NSs, which is larger by an order of magnitude than that for corresponding BH–NS binaries. The masses of the dynamical ejecta owe their difference to the presence/absence of the surface of the heavier NS, which allows the material of the disrupted lighter component to be ejected before the whole system collapses into the remnant BH (see also Kiuchi et al. 2019). While these models are not directly comparable to GW190425, our results suggest that the dynamical ejecta of $\gtrsim 10^{-3} M_{\odot}$ was possible if GW190425 was asymmetric binary NSs, particularly if the NS radius is $\gtrsim 12$ km.

To summarize, the dynamical ejecta are very tiny for low-mass BH–NS binaries, while they could be $\gtrsim 10^{-3} M_{\odot}$ for asymmetric and massive binary NSs. By contrast, the disk mass can be as large as ~ 0.05 – $0.1 M_{\odot}$, irrespective of the binary type unless the NS radius is $\lesssim 11.5$ km. This indicates that the main ejection channel for these systems is likely to be the post-merger disk activity.

3.1.2. Post-merger Phase

It is commonly believed that the outflow from the BH–accretion disk is neutron-rich enough to synthesize abundance of lanthanide elements (e.g., Just et al. 2015; Siegel & Metzger 2018; Fernández et al. 2019). This should be contrasted with the lanthanide-poor outflow from the tori surrounding massive NSs, which emit a copious amount of neutrinos to mitigate neutron richness (Fujibayashi et al. 2018). However, no simulation of the BH–disk outflow has been performed in general-relativistic viscous hydrodynamics. In addition, initial conditions have typically been given without referring to merger simulations (but see also Fernández et al. 2017).

To explore properties of the outflow from the remnant BH–accretion disk, we performed axisymmetric viscous-neutrino-radiation-hydrodynamics simulations in full general relativity (Fujibayashi et al. 2020). Our fiducial models consist of a $0.1 M_{\odot}$ disk surrounding a $3 M_{\odot}$ BH with its dimensionless spin parameter being 0.8 or 0.6. This reasonably models the

merger product of GW190425 for the case of a low-mass BH–NS binary or asymmetric binary NSs (see the previous section for the disk mass).

The simulations show that 15%–30% of the initial disk material is ejected on the timescale of ~ 0.3 – 1 s in a quasi-spherical manner for a plausible range of the alpha viscosity parameter, $\alpha = 0.05$ – 0.15 . This ejection efficiency agrees with that found in previous work (e.g., Just et al. 2015; Siegel & Metzger 2018; Fernández et al. 2019). The outflow is driven by the viscosity, which is presumably induced by magnetoturbulence in realistic situations, and the contribution of neutrino-driven winds is negligible. Because the disk outflow dominates the dynamical ejecta in terms of the mass, properties of the disk outflow primarily determine whether the kilonova/macronova is detectable for a GW190425-like system, irrespective of the binary type.

One crucial difference of our results from previous ones (e.g., Just et al. 2015; Siegel & Metzger 2018; Fernández et al. 2019) is that the electron fraction Y_e of the disk outflow is not very low with its mass-averaged value being ~ 0.3 even in the absence of the strong neutrino emitter, i.e., the remnant NS. This result is rather similar to that of our previous work on accretion tori around massive NSs (Fujibayashi et al. 2018). The reason for this difference is that the mass ejection occurs on the viscous timescale of ~ 0.3 – 1 s as stated above. Because the outflow is not driven significantly until the weak processes freeze out and neutrino cooling becomes inefficient, the disk material typically relaxes to equilibrium of electron/positron captures by the time of ejection. Thus, the neutron richness is mitigated for most of the disk outflow (Fujibayashi et al. 2020). By contrast, if the mass ejection occurs on a short timescale of $\lesssim 0.1$ s, the neutron richness of the ejecta could be high (e.g., Siegel & Metzger 2018; Christie et al. 2019; Fernández et al. 2019).

Post-process nuclear network calculations show that the lanthanide mass fraction, a key parameter to determine the opacity (Kasen et al. 2017; Tanaka et al. 2019), of the disk outflow derived in our simulations, is limited to $\lesssim 10^{-3}$ for $(0 <)\alpha \lesssim 0.1$ (Fujibayashi et al. 2020). The opacity of such lanthanide-poor ejecta is lower by an order of magnitude than the lanthanide-rich case. As a general trend, the lanthanide mass fraction increases as the alpha viscosity parameter increases or the initial mass of the disk decreases. This trend implies that the lanthanide mass fraction can have diversity for a given mass of the outflow, and further case-by-case studies or first-principle neutrino-radiation-magnetohydrodynamics simulations are warranted.

To summarize, the outflow from the BH–accretion disk can be either lanthanide-poor or rich reflecting the timescale of mass ejection. In the following, we consider both cases for assessing the detectability of electromagnetic counterparts. Meanwhile, the ejection efficiency is likely to be 15%–30%.

We note that the similarity of the remnant BH–disk system suggests that possible gamma-ray bursts should also be similar, irrespective of the binary type. However, it is premature to conclude anything about the driving process of an ultrarelativistic jet. We do not discuss the gamma-ray burst here, and it definitely requires future investigation.

3.2. Kilonova/Macronova

To assess the detectability, we computed multiband light curves of the kilonova/macronova associated with various

possible configurations of ejecta from GW190425-like systems by Monte-Carlo radiation-transfer simulations with the code developed in Tanaka & Hotokezaka (2013) and Kawaguchi et al. (2019), and the line list described in Tanaka et al. (2019). The density profile and anisotropy of the dynamical ejecta are modeled following Kawaguchi et al. (2019). The mass-averaged velocity of the disk outflow is varied from 6% to 10% of the speed of light, and the following discussion does not depend on the specific choice. It should be cautioned that predictions of the kilonova/macronova depend on computational methods and systematic errors should be mitigated by cross comparisons with other models (see e.g., Kasen et al. 2017; Bulla 2019; Coughlin et al. 2020).

The results are summarized in Figure 1 for two representative viewing angles with incorporating distance uncertainties, which depend on the viewing angle via the correlation in determining gravitational-wave amplitude (Abbott et al. 2020). Specifically, the distance should be larger for more polar direction, and vice versa, for given amplitude. We explain individual cases below.

Our simulations indicate that a survey equivalent to Coughlin et al. (2019) is likely to detect the emission from the disk outflow if it is lanthanide poor (see the top row of Figure 1). Specifically, for the material with $Y_e = 0.3\text{--}0.4$, the emission at 1 day after merger reaches ~ 20 mag in the r/g -bands for a hypothetical distance of 150 Mpc. Indeed, the emission reaches 21 mag even if the mass is reduced to $0.01 M_\odot$. Thus, if the non-detection of Coughlin et al. (2019) had really covered the location of GW190425, neither a low-mass BH–NS binary nor asymmetric binary NSs is preferred unless a small NS radius of $\lesssim 11.5$ km suppresses the disk formation. Although the dynamical ejecta with $\gtrsim 10^{-4} M_\odot$ could conceal the emission in the equatorial direction by the lanthanide-curtain effect (Kasen et al. 2015) even taking the proximity into account, this applies only to highly equatorial angles of $\gtrsim 75^\circ$ and half of the azimuthal angle due to anisotropy (Kyutoku et al. 2015).

If the disk outflow is lanthanide rich, the detectability depends on the combination of the viewing angle and the amount of the dynamical ejecta (see the bottom row of Figure 1). Specifically, for the material with $Y_e = 0.1\text{--}0.3$, the high opacity renders the emission from the outflow of $0.02 M_\odot$ marginally undetectable 21.5 mag for 150 Mpc. This can be detected from the equatorial direction with a small distance, but not from the polar direction with a large distance. However, the lanthanide-rich dynamical ejecta of $\gtrsim 10^{-4} M_\odot$ associated with a large NS radius of $\gtrsim 12.5$ km interchange the detectability of these two cases. On the one hand, the emission in the polar direction is boosted by 0.5–1 mag and could become detectable. On the other hand, the lanthanide-rich disk outflow is concealed by the lanthanide-rich dynamical ejecta and becomes undetectable in the equatorial direction despite their similar composition. This is ascribed to the low temperature and density of the dynamical ejecta, where the latter increases the expansion opacity as far as the medium is optically thick (see e.g., Equation (1) of Kawaguchi et al. 2019). Because gravitational-wave detections are biased toward polar directions (Schutz 2011), the dynamical ejecta may tend to enhance the detectability.

We caution that enhancement in the polar direction due to the dynamical ejecta is only marginal for the cases relevant to GW190425, particularly taking uncertain microphysics in

radiation-transfer simulations into account (Kawaguchi et al. 2019). For the r -band magnitude to exceed 21 mag significantly for 150 Mpc, dynamical ejecta as massive as $\gtrsim 0.01 M_\odot$ are required, which is comparable to the mass of the disk outflow. Such vigorous dynamical mass ejection is unlikely to occur for low-mass BH–NS binaries. This might be possible with asymmetric binary NSs, whose kilonova/macronova may be characterized by the disk outflow with relatively massive dynamical ejecta.

4. Discussion

Although huge uncertainties are inevitable, we speculate implications of possible future detections of kilonovae/macronovae from GW190425-like events by a survey like Coughlin et al. (2019; see Table 1 for the summary of detectability). Because a successful detection will tell us the host galaxy and its distance, accuracy in determining the viewing angle will be improved by mitigating the degeneracy in the gravitational-wave amplitude (see e.g., Finstad et al. 2018; Mandel 2018, for the case of GW170817). First, if it turns out that we are in the equatorial direction of the event, the dynamical ejecta may be $\lesssim 10^{-4} M_\odot$ for the disk outflow to avoid lanthanide curtains. This case may support the hypothesis of a low-mass BH–NS binary if massive and luminous dynamical ejecta of $\gtrsim 0.01 M_\odot$ are rejected by further follow-up observations. If the dynamical ejecta are massive, asymmetric binary NSs are favored. Second, if we are in the polar direction, the lanthanide-rich disk outflow without dynamical ejecta is not preferred. This may disfavor lanthanide-rich disk outflows after tidal disruption of neutron stars with small radii of $\lesssim 12.5$ km by low-mass BHs. Any detection will not support binary NSs resulting in prompt collapse or a low-mass BH–NS binary with a small NS radius of $\lesssim 11.5$ km, because they leave a negligible amount of material.

If an upper limit of ~ 21 mag is established for a future GW190425-like event, the most likely source may be symmetric binary NSs that collapsed promptly, and a low-mass BH–NS binary may be acceptable only for the following cases (see Table 1 for the summary): (i) it is observed from the equatorial direction, thus close, but the dynamical ejecta associated with a large NS radius of $\gtrsim 12.5$ km concealed the lanthanide-rich disk outflow, and the same applies to the lanthanide-poor disk outflow for highly equatorial directions; (ii) it is observed from the polar direction, thus distant, and early ejection of the lanthanide-rich disk outflow occurs without significant dynamical mass ejection due to a small NS radius of $\lesssim 12.5$ km, or (iii) the disk outflow is suppressed to $\lesssim 0.01 M_\odot$ due to insignificant disk formation associated with a small NS radius of $\lesssim 11.5$ km (see also, e.g., Miller et al. 2019, for preference of a large radius by pulsar observations) or accidentally low ejection efficiency from the disk.

If GW190425-like systems are not very rare, we have a good chance of observing them with the multiple detector network in the near future (Abbott et al. 2018b). The localization error should be improved to the extent that follow-up observations will be able to cover the entire localization area, hopefully deeper. For a hypothetical distance of 150 Mpc consistent with GW190425, the peak magnitude of the kilonova/macronova may reach ≈ 20 mag in the r/g -bands for asymmetric systems, powered mainly by the disk outflow. Thus, observations comparable to Coughlin et al. (2019) will detect the emission or put an informative limit on the possibility of low-mass

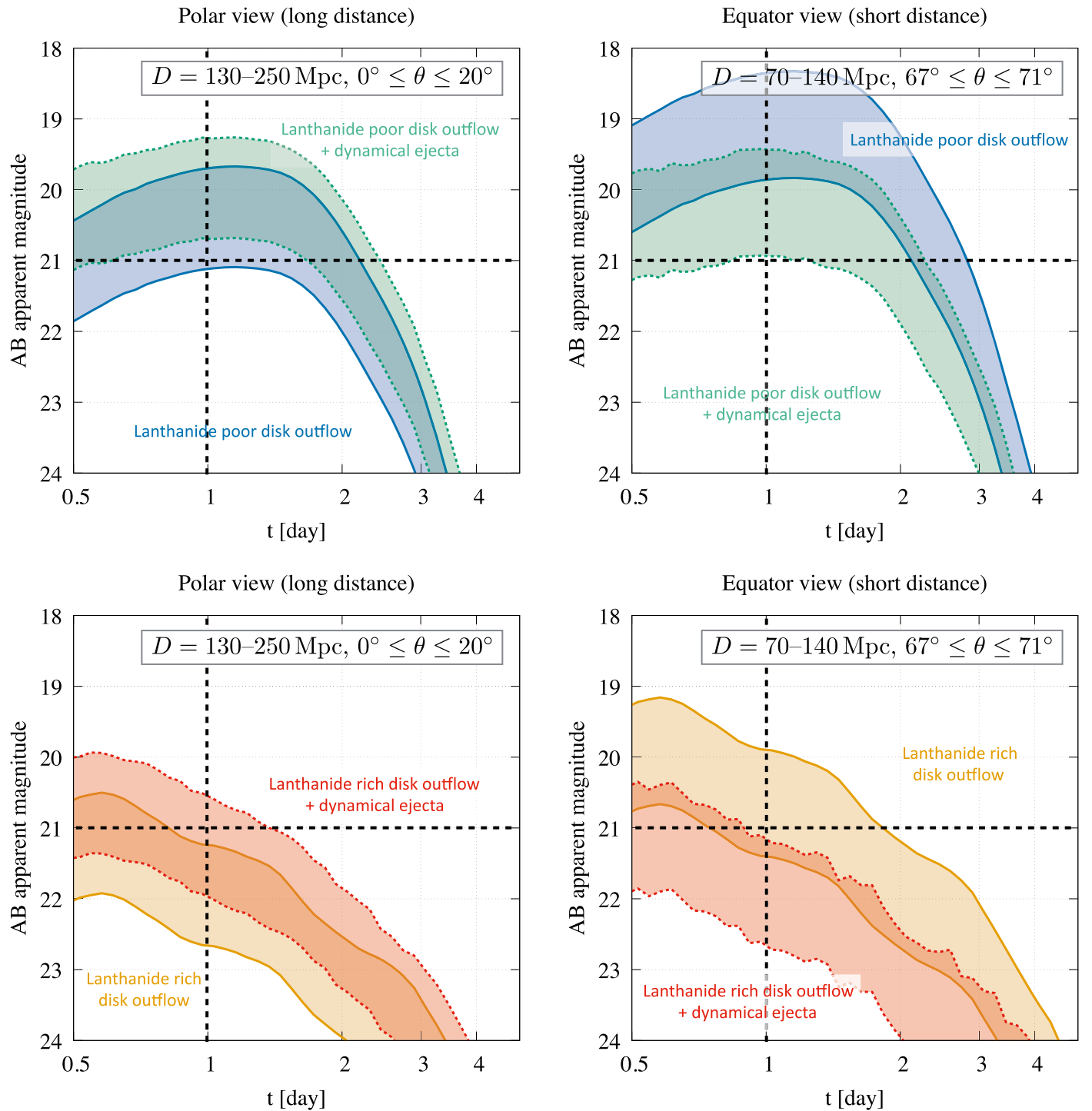


Figure 1. Various possible r -band light curves in AB magnitude of the kilonova/macronova for GW190425-like events. The left and right columns show results for polar viewing angles of $0^\circ\text{--}20^\circ$ from the rotational axis of the binary at 130–250 Mpc and the equatorial one of $67^\circ\text{--}71^\circ$ at 70–140 Mpc, respectively. The distance is matched to GW190425 taking the correlation with the viewing angle into account (Abbott et al. 2020). The blue and green strips in the top panels correspond to the lanthanide-poor disk outflows of $0.02 M_\odot$ without and with dynamical ejecta of $10^{-4} M_\odot$, respectively. The orange and red strips in the bottom panels are the same as above but for the lanthanide-rich disk outflows. Thick dashed lines indicate 21 mag and 1 day (Coughlin et al. 2019).

BH–NS binaries (and asymmetric binary NSs). The multiple detector network also improves the accuracy in the distance and the viewing angle (Cutler & Flanagan 1994). Even if the localization error is not improved due to, e.g., low duty cycle, future sensitive surveys with telescopes like the Vera C. Rubin Observatory (formerly LSST) will be a powerful tool to

detect GW190425-like events. To differentiate binary types with future multi-messenger astronomy, it will be beneficial to improve understanding of the NS equation of state and disk activity. Studies on these topics will also improve phenomenological models of the kilonova/macronova employed in expansive statistical analysis (e.g., Coughlin et al. 2019, 2020;

Table 1

Detectability of the Kilonovae/Macronovae from GW190425-like Events with Respect to the Binary Type and the Merger Outcome

Binary Type	Merger Outcome ^a	Detectable? ^b
low-mass BH–NS	La-poor disk	YES
	La-poor disk+La-rich dyn.	≈YES
	La-rich disk	YES if equatorial
	La-rich disk+La-rich dyn.	YES if polar
	weak/no disruption (small radius)	NO
asymmetric NS–NS	La-poor disk+La-rich dyn.	YES if polar
	La-rich disk+La-rich dyn.	YES if polar
symmetric NS–NS	massive NS (large maximum mass)	YES if polar
	prompt collapse	NO

Notes. Parentheses in the “Merger Outcome” column indicate the required NS properties. Any binary type becomes trivially undetectable if the ejection efficiency happens to be low.

^a La-rich: lanthanide rich; La-poor: lanthanide poor; disk: disk outflow of $\sim 10^{-2} M_{\odot}$; dyn.: dynamical ejecta of $\gtrsim 10^{-4} M_{\odot}$.


^b ≈YES: except for highly equatorial directions heavily obscured by lanthanide curtains; polar: observed from the polar direction avoiding lanthanide curtains; equatorial: observed from the equatorial direction with a small distance.

Coughlin & Dietrich 2019; Hinderer et al. 2019), which will play an important role for quantitative inferences of source properties.

Numerical computations were performed at Oakforest-PACS at Information Technology Center of the University of Tokyo, Cray XC50 at CfCA of National Astronomical Observatory of Japan, Cray XC40 at Yukawa Institute for Theoretical Physics of Kyoto University, and Sakura and Cobra clusters at Max Planck Computing and Data Facility. This work is supported by Japanese Society for the Promotion of Science (JSPS) KAKENHI grant No. JP16H02183, No. JP16H06342, No. JP17H01131, No. JP18H01213, No. JP18H04595, No. JP18H05236, and No. JP19K14720.

ORCID iDs

Koutarou Kyutoku  <https://orcid.org/0000-0003-3179-5216>

Kenta Kiuchi  <https://orcid.org/0000-0003-4988-1438>

Masaru Shibata  <https://orcid.org/0000-0002-4979-5671>

Masaomi Tanaka  <https://orcid.org/0000-0001-8253-6850>

References

Abbott, B. P., Abbott, R., Abbott, T. D., et al. 2017a, *Natur*, 551, 85
 Abbott, B. P., Abbott, R., Abbott, T. D., et al. 2017b, *ApJL*, 848, L13
 Abbott, B. P., Abbott, R., Abbott, T. D., et al. 2017c, *PhRvL*, 119, 161101
 Abbott, B. P., Abbott, R., Abbott, T. D., et al. 2017d, *ApJL*, 848, L12
 Abbott, B. P., Abbott, R., Abbott, T. D., et al. 2018a, *PhRvL*, 121, 161101
 Abbott, B. P., Abbott, R., Abbott, T. D., et al. 2018b, *LRR*, 21, 3
 Abbott, B. P., Abbott, R., Abbott, T. D., et al. 2019a, *PhRvX*, 9, 031040
 Abbott, B. P., Abbott, R., Abbott, T. D., et al. 2019b, *PhRvL*, 123, 011102
 Abbott, B. P., Abbott, R., Abbott, T. D., et al. 2020, arXiv:2001.01761
 Akmal, A., Pandharipande, V. R., & Ravenhall, D. G. 1998, *PhRvC*, 58, 1804
 Andreoni, I., Goldstein, D. A., Kasliwal, M. M., et al. 2019, arXiv:1910.13409
 Arcavi, I., Hosseinzadeh, G., Howell, D. A., et al. 2017, *Natur*, 551, 64
 Bulla, M. 2019, *MNRAS*, 489, 5037
 Christie, I. M., Lalakos, A., Tchekhovskoy, A., et al. 2019, *MNRAS*, 490, 4811

Coughlin, M. W., Ahumada, T., Anand, S., et al. 2019, *ApJL*, 885, L19
 Coughlin, M. W., & Dietrich, T. 2019, *PhRvD*, 100, 043011
 Coughlin, M. W., Dietrich, T., Antier, S., et al. 2020, *MNRAS*, 492, 863
 Coughlin, M. W., Dietrich, T., Margalit, B., & Metzger, B. D. 2019, *MNRAS*, 489, L91
 Coulter, D. A., Foley, R. J., Kilpatrick, C. D., et al. 2017, *Sci*, 358, 1556
 Cromartie, H. T., Fonseca, E., Ransom, S. M., et al. 2020, *NatAs*, 4, 72
 Cutler, C., & Flanagan, É E. 1994, *PhRvD*, 49, 2658
 De, S., Finstad, D., Lattimer, J. M., et al. 2018, *PhRvL*, 121, 091102
 Farrow, N., Zhu, X.-J., & Thrane, E. 2019, *ApJ*, 876, 18
 Fernández, R., Foucart, F., Kasen, D., et al. 2017, *CQGra*, 34, 154001
 Fernández, R., Tchekhovskoy, A., Quataert, E., Foucart, F., & Kasen, D. 2019, *MNRAS*, 482, 3373
 Finstad, D., De, S., Brown, D. A., Berger, E., & Biver, C. M. 2018, *ApJL*, 860, L2
 Foucart, F., Duez, M. D., Kidder, L. E., et al. 2019, *PhRvD*, 99, 103025
 Fujibayashi, S., Kiuchi, K., Nishimura, N., Sekiguchi, Y., & Shibata, M. 2018, *ApJ*, 860, 64
 Fujibayashi, S., Shibata, M., Wanajo, S., et al. 2020, arXiv:2001.04467
 Goldstein, A., Veres, P., Burns, E., et al. 2017, *ApJL*, 848, L14
 Hannam, M., Brown, D. A., Fairhurst, S., Fryer, C. L., & Harry, I. W. 2013, *ApJL*, 766, L14
 Harry, I., & Hinderer, T. 2018, *CQGra*, 35, 145010
 Hinderer, T., Nisanke, S., Foucart, F., et al. 2019, *PhRvD*, 100, 063021
 Hosseinzadeh, G., Cowperthwaite, P. S., Gomez, S., et al. 2019, *ApJL*, 880, L4
 Hotokezaka, K., Kiuchi, K., Kyutoku, K., et al. 2013, *PhRvD*, 87, 024001
 Hotokezaka, K., Kyutoku, K., Okawa, H., Shibata, M., & Kiuchi, K. 2011, *PhRvD*, 83, 124008
 Just, O., Bauswein, A., Pulpillo, R. A., Goriely, S., & Janka, H.-T. 2015, *MNRAS*, 448, 541
 Kasen, D., Fernández, R., & Metzger, B. D. 2015, *MNRAS*, 450, 1777
 Kasen, D., Metzger, B., Barnes, J., Quataert, E., & Ramirez-Ruiz, E. 2017, *Natur*, 551, 80
 Kawaguchi, K., Shibata, M., & Tanaka, M. 2019, arXiv:1908.05815
 Kiuchi, K., Kawaguchi, K., Kyutoku, K., et al. 2017, *PhRvD*, 96, 084060
 Kiuchi, K., Kyutoku, K., Shibata, M., & Taniguchi, K. 2019, *ApJL*, 876, L31
 Kiuchi, K., Sekiguchi, Y., Shibata, M., & Taniguchi, K. 2010, *PhRvL*, 104, 141101
 Kreidberg, L., Bailyn, C. D., Farr, W. M., & Kalogera, V. 2012, *ApJ*, 757, 36
 Kyutoku, K., Ioka, K., Okawa, H., Shibata, M., & Taniguchi, K. 2015, *PhRvD*, 92, 044028
 Kyutoku, K., Kiuchi, K., Sekiguchi, Y., Shibata, M., & Taniguchi, K. 2018, *PhRvD*, 97, 023009
 Lackey, B. D., Kyutoku, K., Shibata, M., Brady, P. R., & Friedman, J. L. 2012, *PhRvD*, 85, 044061
 Li, L.-X., & Paczyński, B. 1998, *ApJL*, 507, L59
 Lipunov, V. M., Gorbvskoy, E., Kornilov, V. G., et al. 2017, *ApJL*, 850, L1
 Mandel, I. 2018, *ApJL*, 853, L12
 Miller, M. C., Lamb, F. K., Dittmann, A. J., et al. 2019, *ApJL*, 887, L24
 Mooley, K. P., Nakar, E., Hotokezaka, K., et al. 2018, *Natur*, 554, 207
 Narikawa, T., Uchikata, N., Kawaguchi, K., et al. 2019, arXiv:1910.08971
 Özel, F., Psaltis, D., Narayan, R., & Villareal, A. S. 2012, *ApJ*, 757, 55
 Pozanenko, A. S., Minaev, P. Y., Grebenev, S. A., & Chelovekov, I. V. 2019, arXiv:1912.13112
 Roberts, L. F., Lippuner, J., Duez, M. D., et al. 2017, *MNRAS*, 464, 3907
 Savchenko, V., Ferrigno, C., Kuulkers, E., et al. 2017, *ApJL*, 848, L15
 Schutz, B. F. 2011, *CQGra*, 28, 125023
 Sesana, A. 2016, *PhRvL*, 116, 231102
 Shibata, M., Kyutoku, K., Yamamoto, T., & Taniguchi, K. 2009, *PhRvD*, 79, 044030
 Shibata, M., Zhou, E., Kiuchi, K., & Fujibayashi, S. 2019, *PhRvD*, 100, 023015
 Siegel, D. M., & Metzger, B. D. 2018, *ApJ*, 858, 52
 Soares-Santos, M., Holz, D. E., Annis, J., et al. 2017, *ApJL*, 848, L16
 Tanaka, M., & Hotokezaka, K. 2013, *ApJ*, 775, 113
 Tanaka, M., Kato, D., Gaigalas, G., & Kawaguchi, K. 2019, arXiv:1906.08914
 Tanaka, M., Utsumi, Y., Mazzali, P. A., et al. 2017, *PASJ*, 69, 102
 Tanvir, N. R., Levan, A. J., González-Fernández, C., et al. 2017, *ApJL*, 848, L27
 Valenti, S., Sand, D. J., Yang, S., et al. 2017, *ApJL*, 848, L24
 Venumadhav, T., Zackay, B., Roulet, J., Dai, L., & Zaldarriaga, M. 2019, arXiv:1904.07214
 Yagi, K., & Yunes, N. 2013, *PhRvD*, 88, 023009
 Yamamoto, T., Shibata, M., & Taniguchi, K. 2008, *PhRvD*, 78, 064054